Prognosis Evaluation Using ^{18}F-Alfatide II PET in a Rat Model of Spinal Cord Injury Treated With Estrogen

Hongpei Tan, PhD[1], Yongxiang Tang, MD[1], Jian Li, MD[1],
Tingting He, MM[2], Ming Zhou, MM[1], and
Shuo Hu, MD, PhD[1,3]

Abstract

Spinal cord injury (SCI) leads to severe dysfunction below injured segment and poses a great pressure to the individual and society. In this study, we applied ^{18}F-alfatide II positron emission tomography/computed tomography (PET/CT) to monitor angiogenesis in an SCI model after estrogen (E2) treatment, as well as to evaluate the prognosis in a noninvasive manner. The SCI model was established with male rats and the rats were randomly divided into E2-treated group (SCI + E2) and E2-untreated group (SCI). Sham group was also used as control (Sham). The angiogenesis after SCI was monitored by ^{18}F-alfatide II PET/CT and verified by immunofluorescence of CD31 and CD61. We also evaluated the level of E2 and growth-associated protein 43 (GAP43) by enzyme-linked immunosorbent assay. Finally, Basso, Beattie, and Bresnahan (BBB) scores were determined to evaluate the exercise capacity of the rats in all 3 groups. Our results showed that the BBB score of SCI + E2 group was significantly different from that of SCI group ($P < .05$) and Sham group ($P < .01$). The uptake of ^{18}F-alfatide II was positively correlated with the expression level of GAP43, both of which reached the peak at day 7 after injury. CD31 and CD61 immunostaining further verified increased angiogenesis in E2-treated SCI lesions. We concluded that ^{18}F-alfatide II PET/CT can monitor the angiogenesis status after SCI in vivo and it may help clinician predict the progression of patients with SCI. This may benefit the study of vascular repair after SCI and provide a tool for evaluation of SCI treatment in clinical practices.

Keywords

PET, integrin $\alpha_v\beta_3$, spinal cord injury, angiogenesis, GAP43

Introduction

Spinal cord injury (SCI) is a catastrophic event which usually happens suddenly and unexpectedly. Spinal cord injury is prevalent in males aged 18 to 32 years in developing countries, leading to severe disability and lethal complications and causing a heavy burden to both the family and the society.[1,2] Spinal cord injury is initiated by a primary injury such as mechanical contusion of the spinal cord, which results in progressive tissue loss. The secondary injury comes from blood vessel dysfunction and inflammation at the epicenter since the milieu of cellular debris and blood at the epicenter is toxic, causing further cell death.[3,4] Neurons are believed to be highly sensitive to such noxious stimuli and are extremely vulnerable to the reductions of perfusion and resultant periods of ischemia.[5] The overall neuronal functions can be compromised by blood vessel loss and disruption of the blood–spinal cord barrier following SCI. The primary injury caused by mechanical damage is irreversible, while the secondary injury is reversible and could be a target for various therapeutic interventions. Therefore, intensive investigations are focused on mechanisms of limiting secondary injury from SCI, such as apoptosis, inflammation,

[1] PET Center of Xiangya Hospital, Central South University, Changsha, Hunan, China
[2] Department of Radiology, Xiangya Hospital, Central South University, Changsha, Hunan, China
[3] National Clinical Research Center for Geriatric Disorders (XIANGYA), Changsha, Hunan, China

Corresponding Author:
Shuo Hu, PET Center of Xiangya Hospital, Central South University, No.87 Xiangya Road, Changsha, Hunan 410000, China.
Email: hushuo2018@163.com

excitotoxicity, and reactive oxygen species generation,[6,7] aiming to achieve 2 major goals: revascularization and axonal regeneration. Although some positive effects for SCI recovery have been reported, more research is needed to truly meet the needs of the clinic. Thus, more effective strategies that can promote functional neurological recovery are in urgent need for SCI treatment.

Studies have shown that female animals behaved significantly better than males in terms of recovering from injury.[8,9] It has been found that estrogen (E2), progesterone, and their metabolites could affect the outcome of traumatic encephalopathy and SCI.[10] Estrogen effectively interfered and reduced the expression of several inflammasomes after SCI and thereby reduced local inflammation in the spinal cord.[11] Samantaray et al found that treatment with E2 could enhance locomotor function recovery by promoting angiogenesis in chronic SCI.[12] The newly formed vessels can provide not only blood supply to the lesioned spinal cord but also the scaffold for the axon crossing the lesions to promote the regeneration of the axon.[13] Therefore, the neoangiogenesis within the lesions may reflect the regeneration of axons and thus could be used as a marker to predict the progression.

Because of the particularity of the spinal cord, noninvasive monitoring strategy is necessary. Since it is very challenging to use morphological imaging modalities such as computed tomography (CT) and magnetic resonance imaging (MRI) to monitor the neovascularization, new methods to monitor angiogenesis in vivo after SCI are needed. Positron emission tomography (PET)/CT has been used as a high-end imaging tool for functional imaging and prognostic evaluation. Recently, several studies applied PET/CT for evaluation of spinal cord energy metabolism.[14,15] Because energy metabolism is affected by many factors, so fluorodeoxyglucose is not an ideal imaging agent after SCI. Research has found that CD61 ($\alpha_v\beta_3$ integrin) plays a key role in endothelial cell survival and migration during angiogenesis. It is highly expressed in activated neovascularization endothelial cells but is low expressed in dormant endothelial cells as well as most tissues and organs,[16–18] so it can be used as a biomarker for new blood vessels formation or existence. Our previous study showed that ^{18}F-alfatide II (^{18}F-AlF-NOTA-e[PEG4-c(RGDfk)]$_2$) PET-targeted CD61 could detect angiogenesis after myocardium infarction and provided a noninvasive way for therapeutic response monitoring.[19]

Growth-associated protein 43 (GAP43) is a neuron-specific phosphoprotein widely existing in nerve tissue, which plays an important role in the growth, differentiation, regeneration of nerve fibers, as well as in growth of axons and formation of synapses.[20] The increased expression of GAP43 after injury has been considered by most researchers to be actively involved in axonal regeneration.[21,22] Herein, with a rat SCI model treated with E2, we used GAP43 expression level as indicator for axonal recovery. We also applied ^{18}F-alfatide II PET to monitor the angiogenesis in the spinal cord after injury. The correlation between angiogenesis determined by PET and axonal recovery was further explored to evaluate the ability of ^{18}F-alfatide II PET in progression prediction.

Materials and Methods

Animals and Surgery

Adult male Sprague-Dawley rats (7 weeks; ~250 g) were used in this research. All procedures of animal experiments were approved by the Ethics Committee of Central South University and were according to the guidelines of the National Institutes of Health on the care and use of animals. A T10 contusive SCI was generated using the modified Allen's impact method. Briefly, all animals were deeply anesthetized by intraperitoneal injection of 3% sodium pentobarbital (0.2 mL/100 g). The vertebral column was exposed between T9 and T10 and a total laminectomy was performed at T10 level. Then the exposed vertebral column was stabilized, the dorsal surface of the spinal cord received an impact of 8 g weight dropping from 40 mm height. Emergence of the immediate intramedullary hemorrhage, pendulous swinging of the tail, and convulsive retraction of both hindlimbs indicated successful establishment of the SCI rat model. After the SCI procedure, animals were housed in individual cages and bladder evacuation was performed daily until they recovered the function. The Sham group received all the described procedures, except for SCI induction. At 3, 7, and 14 days, 4 rats were taken from each group for imaging and then these rats were killed for histological verification; on day 28, the remaining 3 rats in each group were scored and killed. No rats were replaced.

Hormone Treatment

17β-Estradiol (E2) was purchased from Sigma-Aldrich and initially dissolved in ethanol and further diluted in sesame oil to obtain final steroid concentrations for the experiment. Spinal cord injury rats were randomly divided into treatment (SCI + E2) group (n = 15), control (SCI) group (n = 15), and Sham group (n = 15). In treatment group SCI + E2, E2 (25 μg/kg body weight) was given subcutaneously as neck depots (~500 μL) immediately after SCI and every 12 hours thereafter up to 72 hours after injury.[23] The rats in the control group (n = 15) received vehicle only (sesame oil plus ethanol as solvent).

Basso, Beattie, and Bresnahan Scoring

Functional recovery after SCI was determined at 1, 3, 7, 14, and 28 days postinjury by 2 independent and well-trained testers blinded to treatment, using open-field overground locomotor performance according to Basso, Beattie, and Bresnahan (BBB) scores.[24,25]

Small Animal PET Scan and MRI

At 3, 7, and 14 days after SCI, the rats were anesthetized using 1.5% sodium pentobarbital (0.2 mL/100 g), and micro-PET scan was acquired for 15 minutes, starting at 1 hour after an intravenous injection of approximately 37 MBq (1 mCi) of ^{18}F-alfatide II. Image acquisitions were performed using a

micro-PET scanner (Mediso, Hungary). The body temperature was maintained using a heating pad throughout the imaging procedures. For each scan, damaged area activity was measured by delimiting 3-dimensional (3-D) volume of interest (VOI). First, we separated the spinal cord by software on the image and then we selected the 3 segments centered on the lesion as the damage segment. More than 2 cm from the damage section is the normal section. The mean standard uptake value of lesion (LSUVmean) was measured by delimiting a cylindrical volume of interest in the damaged segment of the spinal cord region. Background activity (SUVmean) was measured by delimiting a cylindrical VOI in the normal segment of the spinal cord. Target to background ratio (TBR) was calculated by dividing LSUVmean by SUVmean. At 3, 7, and 14 days after SCI, the rats were anesthetized and T2-weighted MRI was acquired using a 3.0 T magnetic resonance scanner (Siemens, Guangdong, China).

Histology

Immediately after killing, the rats were perfused transcardially with phosphate-buffered saline (PBS) followed by 4% paraformaldehyde in 0.1 M phosphate buffer (pH 7.4). Subsequently, the spinal cords were carefully dissected out and 10-mm segments containing the injury site were postfixed for 24 hours at 4°C. Then the spinal cords were cryoprotected in 20% sucrose in 0.1 M PBS at 4°C until further processing.

Distribution of ^{18}F-Alfatide II in Injured Spinal Cord

After the rats were killed, the spinal cord segment with a length of 1 cm long was harvested and centered by treated segment, wet-weighed, and counted in an Automatic Gamma Counters (PerkinElmer Instruments, Inc, Waltham, Massachusetts). The radioactivity of the tissue samples was converted to the percent injected dose per gram (%ID/g) after calibration.

Immunofluorescence Staining

After fixation, the spinal cords were embedded and frozen in CRYO-OCT compound (Tissue-Tek, Torrance, California) and then sectioned into slices of 5 μm in thickness. The slices were fixed with ice-cold acetone for 10 minutes and dried in the air for 30 minutes. Then, the slices were rinsed with PBS for 2 minutes and blocked with 2% bovine serum albumin (BSA) in PBS for 30 minutes at room temperature. The slices were then incubated overnight at 4°C with mouse anti-rat CD31 (1:200, Abcam, San Francisco, California) to trace the resting endothelial cells or CD61 antibody (1:200, Abcam) to trace the activated neovascular endothelial cells. Then, the slices were incubated with Cy3 and immunoglobulin G-conjugated secondary antibody (1:600, Abcam) for labeling. After 3 more washes with PBS, the slides were stained for nuclei with 4′,6-diamidino-2-phenylindole (DAPI). The immunofluorescence staining was observed under an epifluorescence microscope. Staining against βIII tubulin was performed with anti-βIII tubulin antibody (1:200, Abcam) and corresponding secondary antibody (1:600, Abcam). Ten random visual field areas within 500 μm around the damage center were selected for quantification. The fluorescence was quantified with the software of image-Pro Plus 6.0.

Measurement of Serum Sex Hormone Levels

Blood samples were collected from the caudal vein and centrifuged for approximately 20 minutes at 3000 rpm within 30 minutes after collection. The supernatants were carefully collected and then stored in −80°C for later testing. The concentration of E2 was measured using corresponding enzyme-linked immunosorbent assay kits (Cusabio Biotech Co, Hubei, China).

Western Blotting

The tissues were homogenized after adding the appropriate amount of RIPA lysis buffer and phenylmethylsulfonyl fluoride and then centrifuged (12 000g, 4°C) for 15 minutes to obtain the supernatant. Equal amounts of lysate proteins (20 μg) were electrophoretically separated by sodium dodecyl sulfate-polyacrylamide gel electrophoresis and transferred to polyvinylidene fluoride membranes. Membranes were blocked in Tris-buffered saline with Tween 20 supplemented with 5% BSA at room temperature for 90 minutes and incubated at 4°C overnight with primary antibodies. They were then subjected to HRP-conjugated secondary antibodies at room temperature for 1.5 hours and proteins were detected using enhanced chemiluminescence system.

Data Analysis

The data concerning various groups were analyzed by 1-way analysis of variance followed by Tukey post hoc test using GraphPad Prism 5. A P value less than .05 was considered statistically significant.

Results

Estrogen Promotes the Recovery of Motor Function After SCI

The BBB scores of 3 groups of rats after surgery were recorded and compared. Both the SCI group and the SCI + E2 group showed obvious motor dysfunction at the first day. The BBB scores began to differ between the 2 groups on the third day postinjury ($P < .05$) and became more significant at day 7 and afterward ($P < .01$). The motor function of the Sham group was not affected (Figure 1A). Fluorescence staining against βIII tubulin (Figure 1B) showed that the structure of microtubulin was normal in Sham group, while the structure of microtubulin in the damaged area of SCI groups was seriously damaged. In SCI + E2 group, the structure of microtubulin can be seen to be repaired as a bridge within the lesion area, providing the morphological evidence of the motor function recovery in SCI + E2 group.
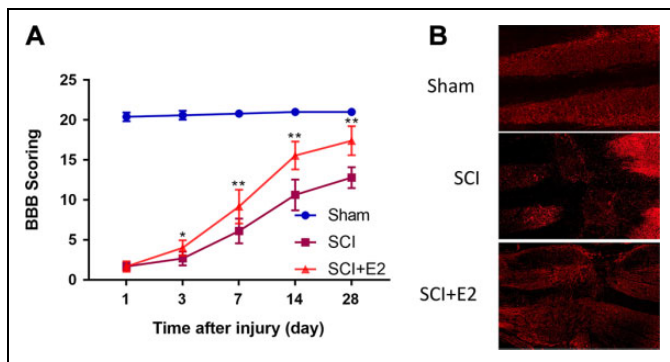
Figure 1. A, BBB scoring at 1, 3, 7, 14, and 28 days postinjury. The significant improvement in motor function was observed in the estrogen treatment group in comparison with SCI without estrogen treatment group from days 3 to 28 postinjury. *$P < .05$, **$P < .01$, SCI + E2 group versus SCI group. B, Immunofluorescence staining of βIII tubulin at day 14 after SCI. Bar = 500 μm. BBB indicates Basso, Beattie, and Bresnahan; SCI, spinal cord injury.

Levels of GAP43 and E2

The results showed that GAP43 began to rise at day 3 after the injury, it became higher on the seventh day and went fell on the 14th day. There was a significant difference between the E2-treated group and the SCI group on day 7 ($P < .01$; Figure 2A). Estrogen levels in the E2-treated group were significantly higher than those in the other 2 groups at day 3 after injury ($P < .001$; Figure 2B).

^{18}F-Alfatide II PET Imaging

To evaluate angiogenesis, PET imaging was performed at 3, 7, 14 days after SCI using ^{18}F-alfatide II as the imaging probe and the results were presented in Figure 3A. No significant tracer uptake was observed in the spinal cord of the rats in the Sham group at all time points, although at day 7, moderate increase in trace uptake was observed out of the scope of the spinal cord. At day 3, increased local tracer uptake was observed in both
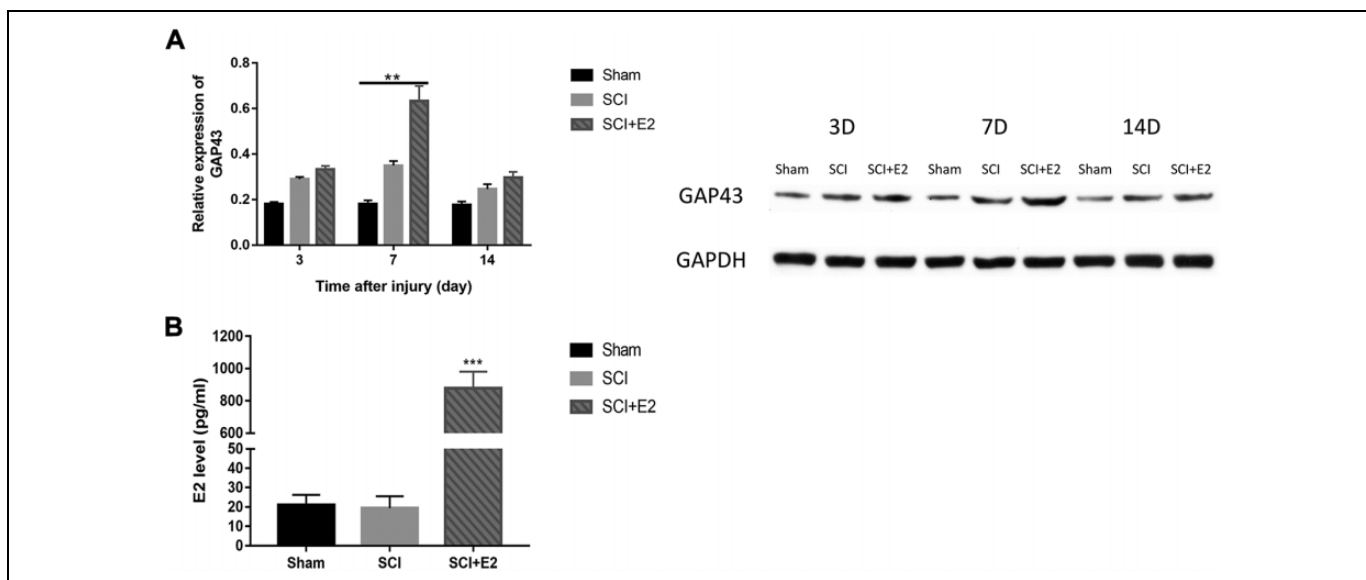
Figure 2. A The GAP43 levels of 3 groups on days 3, 7, and 14 postinjury (**$P < .01$). B, Results of estrogen levels in 3 groups on the third day after injury (***$P < .001$). GAP43 indicates growth-associated protein 43.
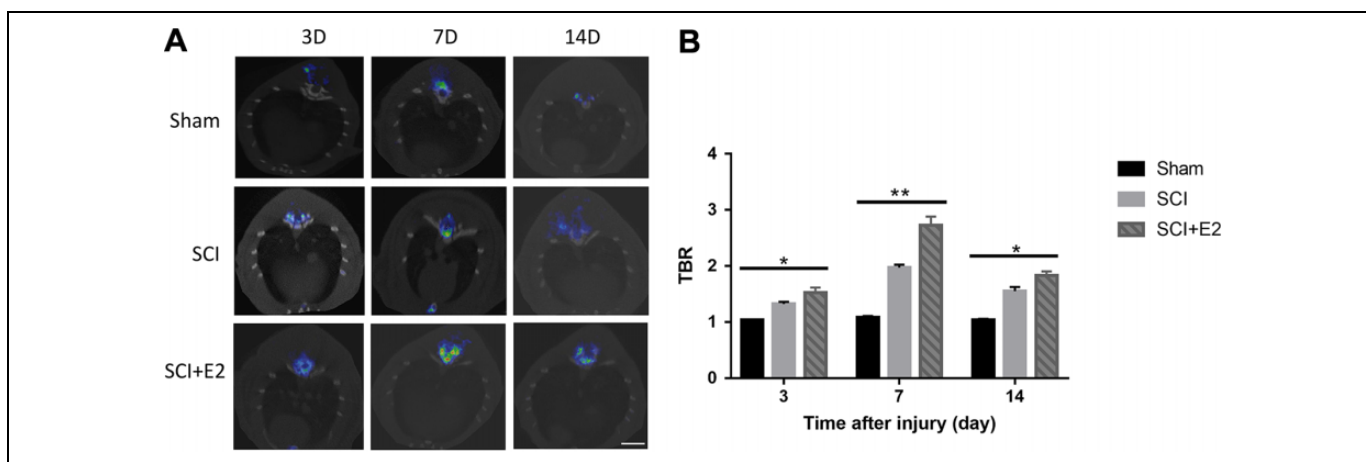
Figure 3. A, 18F-alfatide II positron emission tomography imaging results at days 3, 7, and 14 postinjury in 3 groups. B, Target to background ratio in 3 groups at different time points. *$P < .05$, **$P < .01$. Bar = 1 cm.
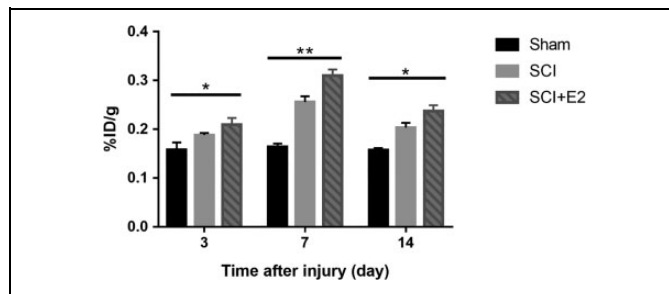
Figure 4. Histogram of the ^{18}F-alfatide II uptake of 3 groups' spinal cord at 3 time points. *P < .05, **P < .01.

SCI and SCI + E2 groups, compared with that in Sham group. At day 7, obvious increased tracer uptake was seen locally at the injured region of spine cord with more intense signal in the SCI + E2 group. The tracer uptake was also shown at day 14 postinjury in both groups, but it was slightly weaker than that at day 7. No differences in tracer uptake between groups were detected in any other regions. All PET images are captured at the highest uptake of imaging agent. We compared the TBR values of the SCI and SCI + E2 groups by outlining VOI (Figure 3B). We can find that the difference on the seventh day was the largest either the visual sense of the image or by analyzing the TBR values.

Distribution of ^{18}F-Alfatide II in Injured Spinal Cord

The tracer uptake ratio of the injured spinal cord is shown in Figure 4. It provides a reference for PET images. At day 3, increased tracer uptake was observed in both SCI and SCI + E2 groups compared with that in Sham group. At day 7, the uptake of tracer became higher in both SCI and SCI + E2 groups and it fell on the 14th day. There were significant differences in 3 groups at 3 time points.

CD31 and CD61 Immunostaining

To further investigate the mechanism of increased tracer uptake after SCI, we performed immunostaining of CD31 (Figure 5) and CD61 (Figure 6) to follow the changes of microvasculature and integrin β3 expression at different time points after SCI. The Sham group was not listed. The expression of CD31 increased along with time in both SCI and SCI + E2 groups. The increase is more apparent in SCI + E2 group than that in SCI group. The fluorescence signal of CD61 was strongest in both SCI and SCI + E2 groups at day 7. The expression of CD61 in SCI + E2 groups was higher than that in SCI group by software quantification.

Results of MRI

T2-weighted MRI was performed to evaluate the injury in both SCI and SCI + E2 groups at 3, 7, and 14 days after SCI (Figure 7). The image showed local edema of rats after SCI, and it can be seen that the edema slowly diminishes over time in both SCI and SCI + E2 groups. There was no statistical difference between SCI and SCI + E2 group.

Discussion

Recent studies have found that angiogenesis and repair of blood vessels after SCI are essential for the recovery of motor function.[26,27] Stem cells or cytokines such as basic fibroblast growth factor, platelet-derived endothelial cell growth factor, transforming growth factor, and vascular endothelial growth factor (VEGF) are now commonly used to promote angiogenesis.[28,29] Mancarella et al[30,31] applied adenovirus loaded with VEGF for promoting angiogenesis and axonal regeneration. However, due to the complexity of procedure and other uncertain factors during application, it was not fully accepted for clinical practice, microRNAs have also been studied in SCI,[32–34] but further research is needed from clinical transformation. Earlier studies have found that women recovered better than men after SCIs.[35] Further research indicated that E2 could reduce inflammation and protect nerve function. Because E2 is readily available and has fewer side effects, it has great potential as a treatment for post-traumatic neuroprotection. In animal studies, E2 has been shown to promote neurofunctional recovery by reducing inflammation and promoting angiogenesis.[11,12,36]

Assessing vascular conditions after SCI is very important for the progression evaluation. CD31 histological immunofluorescence staining is conventionally used in many studies to evaluate vascular structure and function, but this method is invasive and only provides a 2-D image of a regenerative vessel. Some researchers performed 3-D imaging of the blood vessels after SCI by using Synchrotron radiation imaging to provide a complete picture of blood vessels after SCI.[37] However, this method is only limited to preclinical studies. In clinical practice, we can only use noninvasive methods to study patients with SCI. Hence, in this study, we used T2-weighted MRI to evaluate the status of spinal cord after injury since it is most commonly used in clinical practice. However, only the regression of spinal cord edema can be observed. Nowadays, many advanced MRI techniques have been developed for spinal cord imaging such as functional MRI, diffusion-weighted imaging, diffusion-tensor imaging, as well as MR spectroscopy. These MRI methods can only assess the integrity and edema of the spinal cord, but not the vascular conditions that are critical to injury recovery. As a powerful imaging tool, PET/CT showed broad applications in both preclinical studies and clinical practice. For example, ^{18}F-GE-180 PET has been applied to monitor neuroinflammation after SCI although the imaging results did not correlate well with the prognosis.[38]

In this study, we demonstrated the proangiogenic effect of E2 in a rat model of SCI. Moreover, we also verified that E2 could promote the recovery of motor function after SCI in rats. The BBB score of SCI + E2 group was significantly different from that of SCI group (P < .05) and Sham group (P < .01). ^{18}F-alfatide II PET scan showed that the tracer uptake in SCI + E2 group is significantly different from that in SCI group at
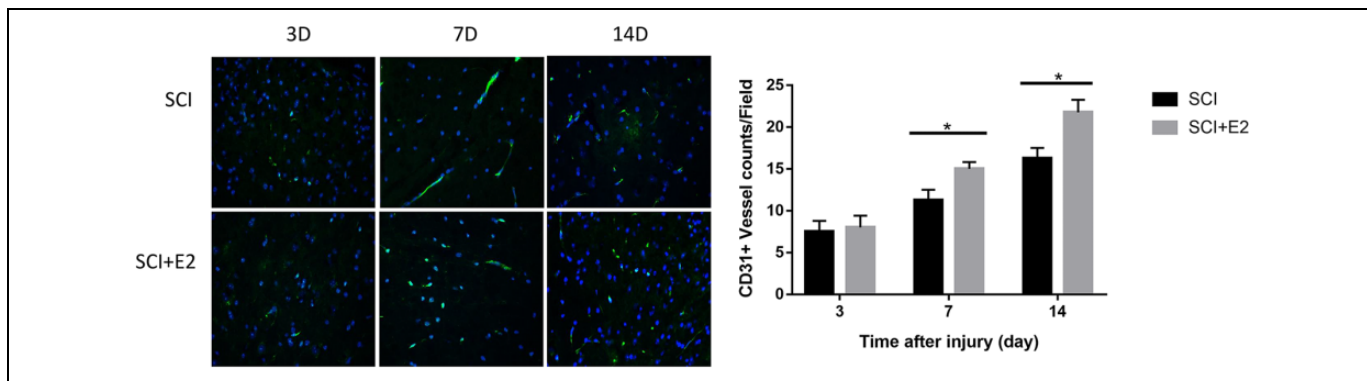
Figure 5. Immunofluorescence staining of CD31 (green). The counts of CD31+ vessel was analyzed (*P < .05). Bar = 50 μm.
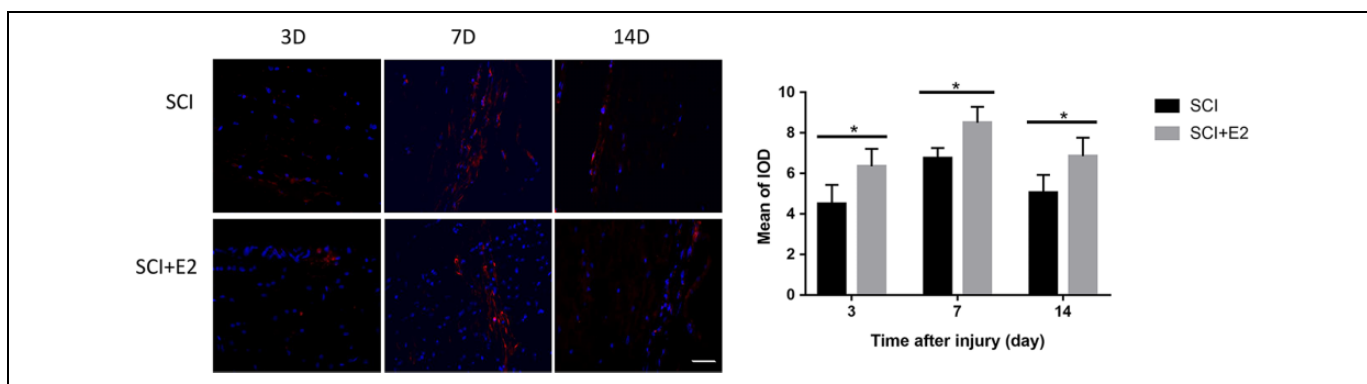
Figure 6. Immunofluorescence staining of CD61 (red). The quantitation analysis was presented in charts (*P < .05). Bar = 50 μm.
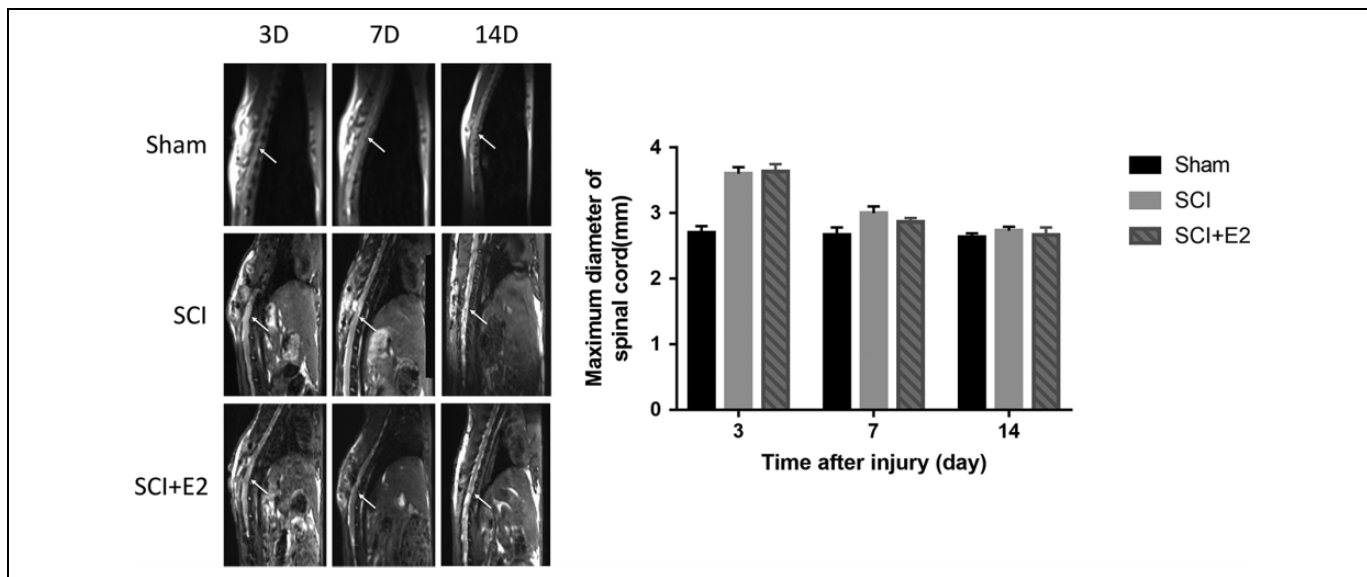
Figure 7. T2-weighted MRI at days 3, 7, and 14 postinjury in SCI rats. The chart shows the maximum diameter of the spinal cord at the lesion. MRI indicates magnetic resonance imaging; SCI, spinal cord injury.

days 3, 7, and 14 postinjury (P < .05). CD31 and CD61 immunostaining further verified increased angiogenesis in E2-treated SCI lesions. Further quantitative analysis of PET images revealed that the difference between the 2 groups was most significant at day 7 after SCI (P < .01) and the tracer uptake ratio of injured spinal cord in vitro verified the results of PET

imaging. We also tested the expression level of GAP43 in 3 groups of rats. By comparing SCI + E2 and SCI group, we found that there was no significant difference between the 2 groups on day 3 and day 14, but there was a significant difference on day 7, indicating that angiogenesis can be used a maker to reflect the regeneration of axons. Because the regeneration of axons is directly related to prognosis, we can evaluate the prognosis of SCI by monitoring the angiogenesis after injury. Our results are consistent with the previous study, which has shown that day 7 after SCI was a critical time for the post-traumatic inflammation.[39] Therefore, we believe that day 7 postinjury is a good time point for prognosis prediction via noninvasive imaging of angiogenesis.

There are still many shortcomings in this study: More frequent imaging may allow us to find the best imaging time, which may help to find the best time for treatment. There may be other reasons for the better recovery of females than males, and this will be further studied in the future.

Conclusion

Our results demonstrated that E2 can promote angiogenesis after SCI and thus increasing local blood supply in vivo. This E2-promoted angiogenesis can be monitored and evaluated efficiently by using ^{18}F-alfatide II. As ^{18}F-alfatide II PET has been applied to other diseases in clinical practice,[40] this imaging strategy could be applied to patients with SCI readily. Therefore, ^{18}F-alfatide II PET could provide a noninvasive way of monitoring therapeutic response and predicting the prognosis after SCI in clinical settings. At the same time, ^{18}F-alfatide II PET could be used as an excellent research tool to shed light on the progress and mechanism of postinjury repair.

Declaration of Conflicting Interests

Funding

ORCID iD

Shuo Hu https://orcid.org/0000-0003-0998-8943

References

1. Selvarajah S, Hammond ER, Schneider EB. Trends in traumatic spinal cord injury. *JAMA*. 2015;314(2):1643.
2. Lee BB, Cripps RA, Fitzharris M, Wing PC. The global map for traumatic spinal cord injury epidemiology: update 2011, global incidence rate. *Spinal Cord*. 2014;52(2):110–116.
3. Bramlett HM, Dietrich WD. Progressive damage after brain and spinal cord injury: pathomechanisms and treatment strategies. *Prog Brain Res*. 2007;161(1):125–141.
4. Oudega M. Molecular and cellular mechanisms underlying the role of blood vessels in spinal cord injury and repair. *Cell Tissue Res*. 2012;349:269–288.
5. Ng MT, Stammers AT, Kwon BK. Vascular disruption and the role of angiogenic proteins after spinal cord injury. *Transl Stroke Res*. 2011;2(4):474–491.
6. Kabu S, Gao Y, Kwon BK, Labhasetwar V. Drug delivery, cell-based therapies, and tissue engineering approaches for spinal cord injury. *J Control Release*. 2015;219:141–154.
7. Kjell J, Olson L. Rat models of spinal cord injury: from pathology to potential therapies. *Dis Model Mech*. 2016;9(10):1125–1137.
8. Semple BD, Dixit S, Shultz SR, Boon WC, O'Brien TJ. Sex-dependent changes in neuronal morphology and psychosocial behaviors after pediatric brain injury. *Behav Brain Res*. 2017; 319(2):48–62.
9. Xu X, Cao S, Chao H, Liu Y, Ji J. Sex-related differences in striatal dopaminergic system after traumatic brain injury. *Brain Res Bull*. 2016;124(1):214–221.
10. Olsen ML, Campbell SC, McFerrin MB, Floyd CL, Sontheimer H. Spinal cord injury causes a wide-spread, persistent loss of Kir4.1 and glutamate transporter 1: benefit of 17 beta-oestradiol treatment. *Brain*. 2010;133:1013–1025.
11. Zendedel A, Monnink F, Hassanzadeh G, et al. Estrogen attenuates local inflammasome expression and activation after spinal cord injury. *Mol Neurobiol*. 2018;55(1):1364–1375.
12. Samantaray S, Das A, Matzelle DC, et al. Administration of low dose estrogen attenuates persistent inflammation, promotes angiogenesis, and improves locomotor function following chronic spinal cord injury in rats. *J Neurochem*. 2016;137(4):604–617.
13. Figley SA, Khosravi R, Legasto JM, Tseng YF, Fehlings MG. Characterization of vascular disruption and blood–spinal cord barrier permeability following traumatic spinal cord injury. *J Neurotrauma*. 2014;31(6):541–552.
14. Floeth FW, Stoffels G, Herdmann J, et al. Prognostic value of ^{18}F-FDG PET in monosegmental stenosis and myelopathy of the cervical spinal cord. *J Nucl Med*. 2011;52(9):1385–1391.
15. Garcia-Panach J, Lull N, Lull JJ, et al. A voxel-based analysis of FDG-PET in traumatic brain injury: regional metabolism and relationship between the thalamus and cortical areas. *J Neurotrauma*. 2011;28:1707–1717.
16. Brooks PC, Clark RA, Cheresh DA. Requirement of vascular integrin alpha v beta 3 for angiogenesis. *Science*. 1994;264(1): 569–571.
17. Brooks PC, Montgomery AM, Rosenfeld M, et al. Integrin alpha v beta 3 antagonists promote tumor regression by inducing apoptosis of angiogenic blood vessels. *Cell*. 1994;79(2):1157–1164.
18. Eliceiri BP, Cheresh DA. The role of alpha v integrins during angiogenesis: insights into potential mechanisms of action and clinical development. *J Clin Invest*. 1999;103(9):1227–1230.
19. Cai M, Ren L, Yin X, et al. PET monitoring angiogenesis of infarcted myocardium after treatment with vascular endothelial growth factor and bone marrow mesenchymal stem cells. *Amino Acids*. 2016;48(3):811–820.

20. Smith SE, Figley SA, Schreyer DJ, Paterson PG. Protein-energy malnutrition developing after global brain ischemia induces an atypical acute-phase response and hinders expression of GAP-43. *PLoS One*. 2014;9(1):e107570.

21. Skene JH. Axonal growth-associated proteins. *Annu Rev Neurosci*. 1989;12:127–156.

22. Tetzlaff W, Alexander SW, Miller FD, Bisby MA. Response of facial and rubrospinal neurons to axotomy: changes in mRNA expression for cytoskeletal proteins and GAP-43. *J Neurosci*. 1991;11(8):2528–2544.

23. Dang J, Mitkari B, Kipp M, Beyer C. Gonadal steroids prevent cell damage and stimulate behavioral recovery after transient middle cerebral artery occlusion in male and female rats. *Brain Behav Immun*. 2011;25(4):715–726.

24. Basso DM, Beattie MS, Bresnahan JC. A sensitive and reliable locomotor rating scale for open field testing in rats. *J Neurotrauma*. 1995;12(1):1–21.

25. Basso DM, Beattie MS, Bresnahan JC. Graded histological and locomotor outcomes after spinal cord contusion using the NYU weight-drop device versus transection. *Exp Neurol*. 1996;139(2):244–526.

26. Jing Y, Bai F, Chen H, Dong H. Melatonin prevents blood vessel loss and neurological impairment induced by spinal cord injury in rats. *J Spinal Cord Med*. 2017;40(2):222–229.

27. Hu JZ, Wang XK, Cao Y, et al. Tetramethylpyrazine facilitates functional recovery after spinal cord injury by inhibiting MMP2, MMP9, and vascular endothelial cell apoptosis. *Curr Neurovasc Res*. 2017;14(2):110–116.

28. Mothe AJ, Tator CH. Advances in stem cell therapy for spinal cord injury. *J Clin Invest*. 2012;122(11):3824–3834.

29. Chen D, Zeng W, Fu Y, Gao M, Lv G. Bone marrow mesenchymal stem cells combined with minocycline improve spinal cord injury in a rat model. *Int J Clin Exp Pathol*. 2015;8(10):11957–11969.

30. Lutton C, Young YW, Williams R, Meedeniya AC, Mackay-Sim A, Goss B. Combined VEGF and PDGF treatment reduces secondary degeneration after spinal cord injury. *J Neurotrauma*. 2012;29(5):957–970.

31. Facchiano F, Fernandez E, Mancarella S, et al. Promotion of regeneration of corticospinal tract axons in rats with recombinant vascular endothelial growth factor alone and combined with adenovirus coding for this factor. *J Neurosurg*. 2002;97(2):161–168.

32. Hu J, Zeng L, Huang J, Wang G, Lu H. MiR-126 promotes angiogenesis and attenuates inflammation after contusion spinal cord injury in rats. *Brain Res*. 2015;1608:191–202.

33. Yang Z, Xu J, Zhu R, Liu L. Down-regulation of miRNA-128 contributes to neuropathic pain following spinal cord injury via activation of P38. *Med Sci Monit*. 2017;23:405–411.

34. Huang JH, Cao Y, Zeng L, et al. Tetramethylpyrazine enhances functional recovery after contusion spinal cord injury by modulation of microRNA-21, FasL, PDCD4 and PTEN expression. *Brain Res*. 2016;1648(pt A):35–45.

35. Chan WM, Mohammed Y, Lee I, Pearse DD. Effect of gender on recovery after spinal cord injury. *Transl Stroke Res*. 2013;4(4):447–461.

36. Sribnick EA, Wingrave JM, Matzelle DD, Wilford GG, Ray SK, Banik NL. Estrogen attenuated markers of inflammation and decreased lesion volume in acute spinal cord injury in rats. *J Neurosci Res*. 2005;82(2):283–293.

37. Ni S, Cao Y, Jiang L, et al. Synchrotron radiation imaging reveals the role of estrogen in promoting angiogenesis after acute spinal cord injury in rats. *Spine*. 2018;43(2):1241–1249.

38. Tremoleda JL, Thau-Zuchman O, Davies M, et al. In vivo PET imaging of the neuroinflammatory response in rat spinal cord injury using the TSPO tracer [(18)F]GE-180 and effect of docosahexaenoic acid. *Eur J Nucl Med Mol Imaging*. 2016;43(9):1710–1722.

39. Beck KD, Nguyen HX, Galvan MD, Salazar DL, Woodruff TM, Anderson AJ. Quantitative analysis of cellular inflammation after traumatic spinal cord injury: evidence for a multiphasic inflammatory response in the acute to chronic environment. *Brain*. 2010;133(pt 2):433–447.

40. Luan X, Huang Y, Gao S, et al. (18)F-alfatide PET/CT may predict short-term outcome of concurrent chemoradiotherapy in patients with advanced non-small cell lung cancer. *Eur J Nucl Med Mol Imaging*. 2016;43(13):2336–2342.